nature medicine

A purified membrane protein from *Akkermansia muciniphila* or the pasteurized bacterium improves metabolism in obese and diabetic mice

Hubert Plovier[1], Amandine Everard[1,8], Céline Druart[1,8], Clara Depommier[1,8], Matthias Van Hul[1], Lucie Geurts[1], Julien Chilloux[2], Noora Ottman[3,7], Thibaut Duparc[4], Laeticia Lichtenstein[4], Antonis Myridakis[2], Nathalie M Delzenne[1], Judith Klievink[5], Arnab Bhattacharjee[5], Kees C H van der Ark[3], Steven Aalvink[3], Laurent O Martinez[4], Marc-Emmanuel Dumas[2], Dominique Maiter[6], Audrey Loumaye[6], Michel P Hermans[6], Jean-Paul Thissen[6], Clara Belzer[3], Willem M de Vos[3,5] & Patrice D Cani[1]

Obesity and type 2 diabetes are associated with low-grade inflammation and specific changes in gut microbiota composition[1–7]. We previously demonstrated that administration of *Akkermansia muciniphila* to mice prevents the development of obesity and associated complications[8]. However, the underlying mechanisms of this protective effect remain unclear. Moreover, the sensitivity of *A. muciniphila* to oxygen and the presence of animal-derived compounds in its growth medium currently limit the development of translational approaches for human medicine[9]. We have addressed these issues here by showing that *A. muciniphila* retains its efficacy when grown on a synthetic medium compatible with human administration. Unexpectedly, we discovered that pasteurization of *A. muciniphila* enhanced its capacity to reduce fat mass development, insulin resistance and dyslipidemia in mice. These improvements were notably associated with a modulation of the host urinary metabolomics profile and intestinal energy absorption. We demonstrated that Amuc_1100, a specific protein isolated from the outer membrane of *A. muciniphila*, interacts with Toll-like receptor 2, is stable at temperatures used for pasteurization, improves the gut barrier and partly recapitulates the beneficial effects of the bacterium. Finally, we showed that administration of live or pasteurized *A. muciniphila* grown on the synthetic medium is safe in humans. These findings provide support for the use of different preparations of *A. muciniphila* as therapeutic options to target human obesity and associated disorders.

Akkermansia muciniphila is one of the most abundant members of the human gut microbiota, representing between 1% and 5% of our intestinal microbes[10,11]. We and others recently observed that the abundance of *A. muciniphila* is decreased during obesity and diabetes[2,8] and that higher baseline abundance is significantly associated with the improvement of cardiometabolic parameters in individuals with obesity undergoing caloric restriction[12]. Moreover, we found that daily administration of live *A. muciniphila* grown on a mucus-based medium can counteract the development of high-fat diet (HFD)-induced obesity and gut barrier dysfunction[8], an observation later confirmed by other groups[13,14]. However, the underlying mechanisms of these effects are still unclear. In addition, the current growth requirements of *A. muciniphila* and its oxygen sensitivity[9] render this bacterium unsuitable for human investigations and putative therapeutic opportunities.

Therefore, in HFD-fed mice, we compared the effects of daily administration of *A. muciniphila* grown either on a mucus-based medium (HFD live *Akk* mucus) or a synthetic medium in which mucin was replaced by a combination of glucose, *N*-acetylglucosamine, soy peptone and threonine (HFD live *Akk* synthetic). This medium allowed us to culture *A. muciniphila* with the same efficiency as in the mucus-based medium while avoiding any compounds that are incompatible with human administration. We observed that live *A. muciniphila* treatment tended to reduce HFD-induced body weight and fat mass gain (by about 40–50%). It also tended to improve glucose intolerance and insulin resistance regardless of both growth medium and food intake (**Fig. 1a–g**).

We previously showed that autoclaving *A. muciniphila* abolished its beneficial effects[8]. However, recent investigations suggest that probiotics inactivated by pasteurization for 30 min at 70 °C, a less extreme treatment limiting the denaturation of their cellular

[1]Université catholique de Louvain, Louvain Drug Research Institute, WELBIO (Walloon Excellence in Life sciences and BIOtechnology), Metabolism and Nutrition Research Group, Brussels, Belgium. [2]Division of Computational and Systems Medicine, Department of Surgery and Cancer, Imperial College London, London, UK. [3]Laboratory of Microbiology, Wageningen University, Wageningen, the Netherlands. [4]Institute of Metabolic and Cardiovascular Diseases, I2MC, Inserm, UMR 1048, Toulouse, France. [5]RPU Immunobiology, Department of Bacteriology & Immunology, University of Helsinki, Helsinki, Finland. [6]Pole of Endocrinology, Diabetes and Nutrition, Institut de Recherche Expérimentale et Clinique IREC, Cliniques Universitaires Saint-Luc, Université catholique de Louvain, Brussels, Belgium. [7]Present address: Metapopulation Research Centre, University of Helsinki, Helsinki, Finland. [8]These authors contributed equally to this work. Correspondence should be addressed to P.D.C. (patrice.cani@uclouvain.be).

Received 31 May; accepted 17 October; published online 28 November 2016; doi:10.1038/nm.4236

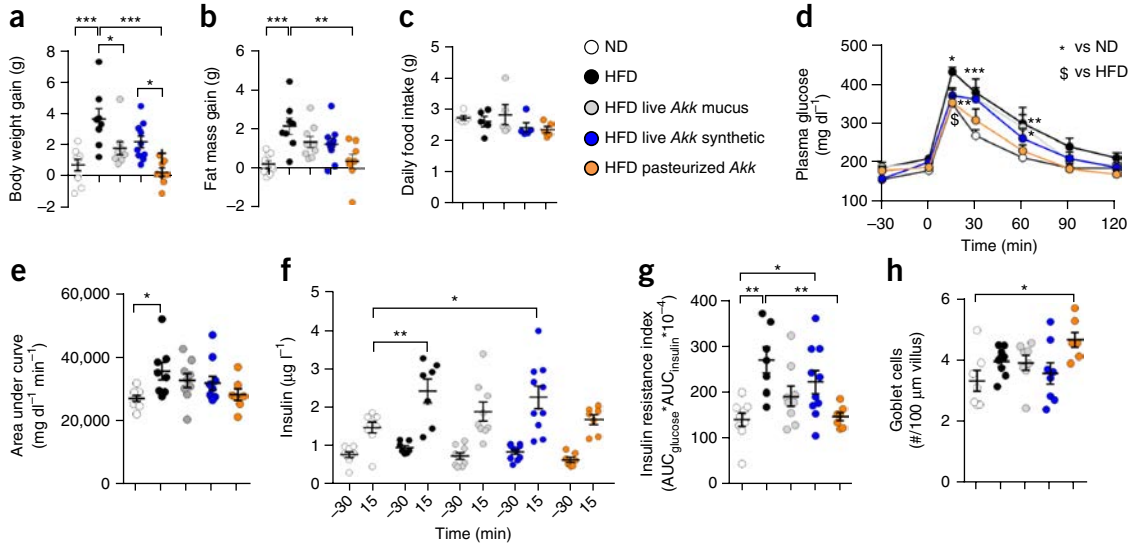

Figure 1 Pasteurization enhances *A. muciniphila*–mediated effects on high-fat diet-induced obesity. (**a**,**b**) Body weight gain (**a**) and fat mass gain (**b**) in grams after 4 weeks of treatment. (**c**) Daily food intake per mouse in grams. (**d**) Plasma glucose (mg dl^{-1}) profile and (**e**) the mean area under the curve (AUC) measured during an oral tolerance test (OGTT) (mg dl^{-1} min^{-1}). (**f**) Plasma insulin (µg l^{-1}) measured30 min before and 15 min after glucose administration during the OGTT. (**g**) Insulin resistance index. (**h**) Ileum goblet cell density. Data are presented as the mean ± s.e.m. Number of mice per group for **a**,**b**: ND: 9, HFD: 8, HFD live *Akk* mucus: 9, HFD live *Akk* synthetic: 10, HFD pasteurized *Akk*: 8. For **c**, 5 measurements were obtained for each group. Number of mice per group for **d**–**g**: ND: 9, HFD: 8, HFD live *Akk* mucus: 9, HFD live *Akk* synthetic: 10, HFD pasteurized *Akk*: 7. Number of mice per group for **h**: ND: 7, HFD: 8, HFD live *Akk* mucus: 8, HFD live *Akk* synthetic: 8, HFD pasteurized *Akk*: 7. Data were analyzed using one-way ANOVA followed by Tukey *post hoc* test for **a**–**c**,**e**,**g**,**h**, and according to two-way ANOVA followed by Bonferroni *post hoc* test for **d**,**f**. $^{*}P < 0.05$; $^{**}P < 0.01$; $^{***}P < 0.001$.

components, could partly or fully retain their beneficial effects[15,16]. Hence, we assessed the effects of *A. muciniphila* grown on a synthetic medium and inactivated by pasteurization (HFD pasteurized *Akk*). Unexpectedly, in two separate sets of experiments, we found that pasteurized *A. muciniphila* exerted stronger effects than the live bacterium independently of food intake, as HFD-fed mice treated with pasteurized bacteria showed similar body weight and fat mass gain to mice fed with a control diet (ND) (**Fig. 1a–c** and **Supplementary Fig. 1a–c**). In both sets of experiments, we found that mice treated with pasteurized *A. muciniphila* displayed a much lower glucose intolerance and insulin concentration when compared to the HFD group, which resulted in a lower insulin resistance (IR) index in the treated mice (**Fig. 1d–g** and **Supplementary Fig. 1d–g**). Treatment with pasteurized *A. muciniphila* also led to greater goblet cell density in the ileum than was found in ND-fed mice (**Fig. 1h**); this suggests that in HFD-fed mice treated with the pasteurized bacterium, as compared to untreated, ND-fed mice, more mucus is produced. Furthermore, when comparing mice treated with pasteurized *A. muciniphila* to untreated, HFD-fed mice, the mean adipocyte diameter (**Fig. 2a**,**b**) is normalized and plasma leptin is significantly lower (**Fig. 2c**). These effects were not observed in mice treated with live *A. muciniphila*. A similar trend was observed for plasma resistin (**Supplementary Fig. 1h**) thereby suggesting improved insulin sensitivity, while plasma adiponectin remained unaffected in all conditions (**Supplementary Fig. 1i**). We found that mice treated with pasteurized *A. muciniphila* had a higher fecal caloric content when compared to all other groups (**Fig. 2d**), suggesting a lower energy absorption. This may further contribute to the reduction in body weight and fat mass gain observed in this group. Similar effects of *A. muciniphila* on energy absorption were previously reported in mice undergoing cold exposure[17]. Altogether, these data suggest that pasteurization enhances the beneficial effects of *A. muciniphila* on HFD-induced metabolic syndrome. This could be due to increased accessibility of specific bacterial compounds that are involved in production of the positive effects of *A. muciniphila* on its host. Conversely, pasteurization of *A. muciniphila* could prevent the production of metabolites or factors that mitigate its beneficial effects.

We next tested whether treatment with *A. muciniphila* could reduce the HFD-induced shift in the host urinary metabolome[18]. HFD was the main factor influencing ^{1}H-NMR-based untargeted metabolic profiles on the first O-PLS-DA score (Tpred1); treatment with pasteurized *A. muciniphila* clustered separately from all other groups regarding the second score (Tpred2) (**Fig. 2e–g**). This resulted in a normalization of the HFD-induced shift of 37% with the pasteurized bacterium and 17% with the live bacterium (**Fig. 2f**).

By comparing the metabolic profiles of the different groups, we found that the shift induced by pasteurized *A. muciniphila* was mainly associated with trimethylamine (TMA) and trimethylamine-*N*-oxide (TMAO) according to the OPLS-DA model coefficients (**Supplementary Fig. 2**). While HFD feeding severely lowered the abundance of TMA compared to ND-fed mice, treatment with pasteurized *A. muciniphila* significantly offset this reduction (**Fig. 2h**). A similar trend was observed for urinary TMAO (**Fig. 2i**). This relative increase in TMA abundance was not observed in mice treated with live *A. muciniphila*. Treatment with pasteurized *A. muciniphila* also modulated hepatic expression of *Fmo3*, a gene encoding flavin monooxygenase 3, which converts TMA to TMAO, a metabolite associated with atherosclerosis[19,20]. While exposure to a HFD led to a two-fold higher *Fmo3* expression as compared to that in ND-fed mice, treatment with pasteurized *A. muciniphila* reversed this effect (**Fig. 2j**). Of note, knockdown of *Fmo3* through the use of specific antisense oligonucleotides can increase serum concentration of TMA[20] and can protect mice against the development of atherosclerosis and insulin resistance[21]. Moreover, recent findings suggest that

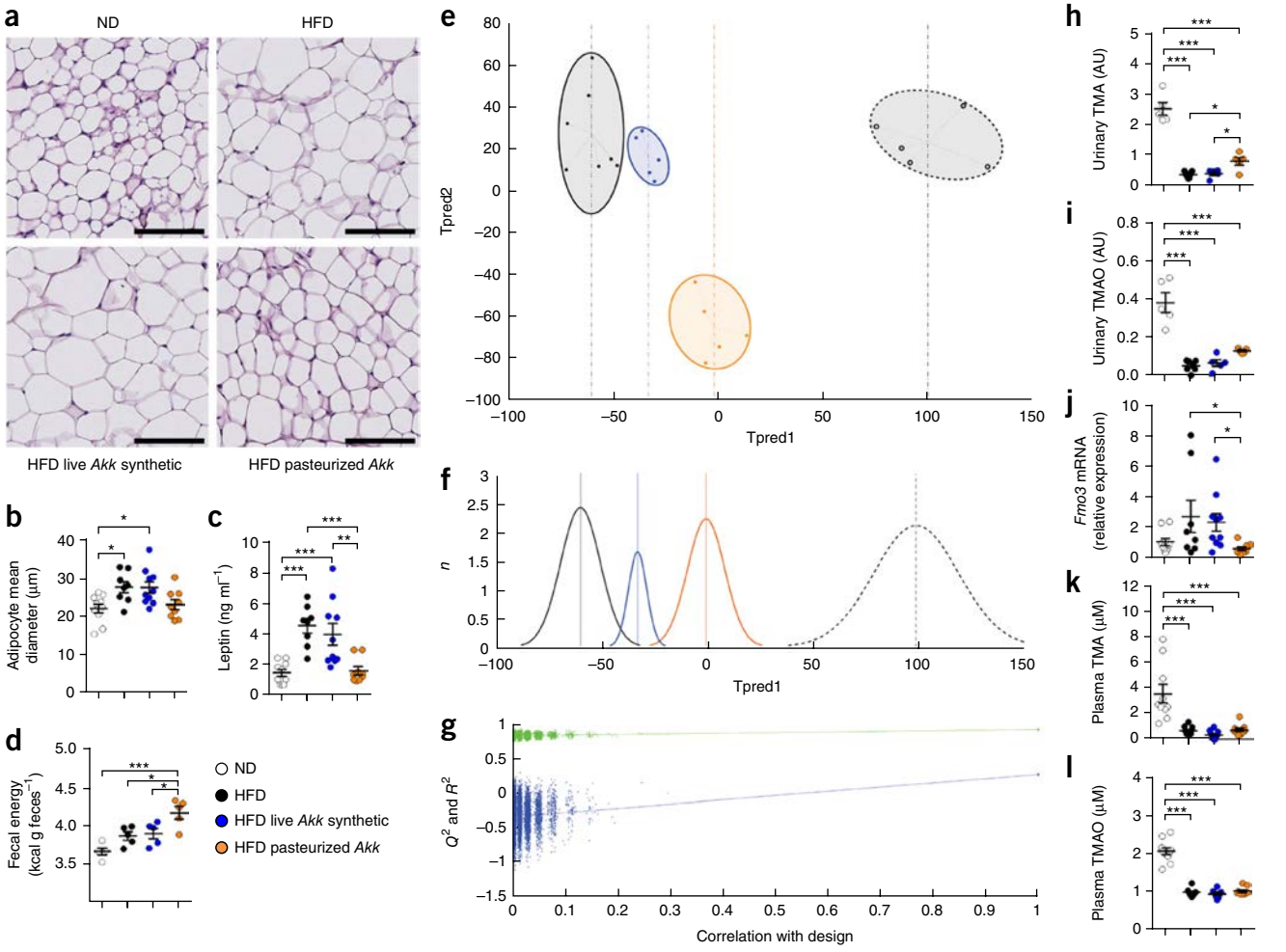

Figure 2 Pasteurized *A. muciniphila* modulates adipose tissue physiology, intestinal energy absorption and urinary metabolome. (**a**) Representative hematoxylin and eosin (H&E)-stained pictures of subcutaneous adipose tissue (SAT) deposits ($n = 5$ images per mouse). Scale bars, 100 µm. (**b**) Mean adipocyte diameter (µm) in the SAT. (**c**) Plasma leptin (ng ml^{-1}). (**d**) Fecal energetic content (kcal g feces^{-1}). (**e**) Orthogonal partial least-squares discriminant analysis (OPLS-DA) predictive score plot for urine metabolic profiles representing predictive component 1 (Tpred1) versus Tpred2. (**f**) Projection of all treatment groups on the first predictive score of the OPLS-DA model. (**g**) Empirical assessment of the significance of O-PLS goodness-of-fit parameters. (**h**,**i**) Relative abundance of urinary (**h**) trimethylamine (TMA) and (**i**) trimethylamine-*N*-oxide (TMAO). (**j**) mRNA expression of hepatic flavin-containing monooxygenase 3. (**k**) Plasma TMA (µM). (**l**) Plasma TMAO (µM). Data are presented as the mean ± s.e.m. Number of mice per group for **a**–**c** and **j**–**l**: ND: 10, HFD: 8, HFD live *Akk* synthetic: 10, HFD pasteurized *Akk*: 9. For **d**, 5 measurements were obtained for each group. Number of mice per group for **e**–**i**: ND: 5, HFD: 7, HFD live *Akk* synthetic: 5, HFD pasteurized *Akk*: 5. Data were analyzed using one-way ANOVA followed by a Tukey *post hoc* test for **b**–**d**, and **h**–**k**. $^{*}P < 0.05$; $^{**}P < 0.01$; $^{***}P < 0.001$.

oral administration of live *A. muciniphila* can impede the development of atherosclerosis in *Apoe*$^{-/-}$ mice[22]. In our study, however, the effects observed on urinary TMA and *Fmo3* expression were not associated with a modification of plasma TMA and TMAO, as all HFD-fed mice displayed similar concentrations for both metabolites (**Fig. 2k**,**l**). This suggests that the observed decrease in *Fmo3* expression is not sufficient to inhibit the conversion of TMA to TMAO, and that the metabolic effects of pasteurized *A. muciniphila* are not related to these two metabolites.

Toll-like receptors (TLRs) regulate bacterial recognition and intestinal homeostasis, and they can also shape the host metabolism[23–25]. To identify how *A. muciniphila* interacts with its host, we performed *in vitro* experiments to evaluate its TLR signaling potential. Previous results suggested that *A. muciniphila* lipopolysaccharide (LPS) differs structurally from that of *Escherichia coli* and is not a powerful TLR4 agonist[26]. Here, we observed that *A. muciniphila* specifically activated cells expressing TLR2 (**Fig. 3a**), but not cells expressing TLR5, TLR9 or the NOD2 receptor (**Fig. 3b**–**d**).

Genomic and proteomic analyses of *A. muciniphila* identified proteins encoded by a specific Type IV pili gene cluster in fractions enriched for outer membrane proteins[27]. Among these, Amuc_1100, a protein of 32 kDa, was one of the most abundant. Additionally, its presence on a gene cluster related to pilus formation suggests that it could be involved in the crosstalk with the host. To test this hypothesis, we showed that a His-tagged Amuc_1100 produced in *E. coli* (hereafter called Amuc_1100*) could signal to TLR2-expressing cells in a similar manner to *A. muciniphila* (**Fig. 3a**). Furthermore, Amuc_1100* appeared relatively thermostable, as differential light scattering analysis indicated its melting temperature was 70° C (**Fig. 3e**), which is the temperature applied for pasteurization. Therefore, Amuc_1100 could still be active in pasteurized bacteria and contribute to the observed signaling.

Consequently, we compared the effects of the live and pasteurized bacterium to those of Amuc_1100* in HFD-fed mice. Similarly to what was observed with the pasteurized bacterium, treatment with Amuc_1100* induced a lower body weight and fat mass gain when compared to that in untreated HFD-fed mice, independently of food intake (**Fig. 3f–h**). It also tended to correct HFD-induced higher adipocyte diameter (**Supplementary Fig. 3a**,**b**). Treatment with *A. muciniphila* or Amuc_1100* corrected HFD-induced hypercholesterolemia with significantly lower plasma HDL cholesterol concentrations; a similar trend was observed for LDL cholesterol (**Fig. 3i**). Mice treated with pasteurized *A. muciniphila* displayed significantly lower plasma triglycerides concentrations than either untreated mice or HFD-fed mice treated with live *A. muciniphila*, again suggesting an increased potency of the bacterium after pasteurization (**Fig. 3j**). No differences were observed in the distribution of triglycerides and cholesterol in lipoproteins (**Supplementary Fig. 3c**,**d**). Amuc_1100* also improved glucose tolerance with the same potency as the live and pasteurized bacterium (**Fig. 3k**,**l**). To further investigate the effects of *A. muciniphila* on insulin sensitivity, we analyzed insulin-induced phosphorylation of the insulin receptor (IR) and its downstream mediator Akt at the threonine (Akt^{thr}) and serine (Akt^{ser}) sites[28] in the liver (**Fig. 3m**,**n**). As previously described, untreated HFD-fed mice displayed lower phosphorylation of all analyzed proteins when compared to ND-fed mice[29], an effect that reached significance for Akt^{thr} (**Fig. 3n**). Treatment with *A. muciniphila* or Amuc_1100* counteracted these effects, with significantly higher levels of p-IR and p-Akt^{thr} in mice treated with Amuc_1100* (**Fig. 3m**,**n**), and significantly higher levels of p-Akt^{ser} in mice treated with the live bacterium (**Fig. 3n**) when compared to untreated HFD-fed mice.

Previous reports show that beneficial effects of *A. muciniphila* are associated with improvements of the gut barrier function[8,13,22,26] leading to a correction of metabolic endotoxemia (i.e., increased portal LPS concentration) in obese and diabetic mice. We therefore assessed the effects of pasteurized *A. muciniphila* and Amuc_1100* on endotoxemia and genes associated with the intestinal barrier. While HFD-fed mice displayed higher portal LPS concentration than ND-fed mice, treatment with *Akkermansia*—either live or pasteurized—or Amuc_1100* completely restored LPS concentration to that observed in the ND group (**Fig. 4a**). Among the assessed markers of the gut barrier, we found that expression of *Cnr1*, coding for cannabinoid receptor 1 (CB_1), was specifically lower in the jejunum of mice treated with Amuc_1100* (**Fig. 4b**). Interestingly, activation of CB_1 was shown to increase intestinal permeability *in vitro*, whereas blocking CB_1 reduces gut permeability both *in vitro* and *in vivo*[30]. In accordance with these findings, genes encoding tight-junction proteins involved in the regulation of intestinal permeability were also affected. In the jejunum, expression of *Cldn3* (encoding claudin 3) was higher in mice treated with Amuc_1100* when compared to untreated HFD-fed mice (**Fig. 4b**); in contrast, expression of *Ocln* (encoding occludin) was higher in all treated groups when compared to ND-fed mice, as well as in mice receiving Amuc_1100* when compared to untreated HFD-fed mice (**Fig. 4b**). In the ileum, a trend for lower *Cnr1* expression was observed following treatment with *A. muciniphila* (**Fig. 4c**). *Cldn3* expression was greater in all treated groups when compared to untreated ND- and HFD-fed mice, while *Ocln* was unaffected (**Fig. 4c**). These effects could notably be explained by the ability of *A. muciniphila* to activate TLR2 via Amuc_1100, as this receptor can regulate various tight-junction proteins including occludin and claudin 3 (refs. 31,32). In the colon, untreated HFD-fed mice had a higher *Ocln* expression as compared to the other groups, whereas *Cnr1* tended to be higher in all HFD-fed groups and *Cldn3* was not modified (**Supplementary Fig. 4a**).

We next assessed markers of the synthesis (*Napepld*) and the degradation (*Naaa*) of different endocannabinoids and bioactive lipids from the *N*-acylethanolamine (NAEs) family[33]. *Napepld* expression was lower specifically in the jejunum following treatment with pasteurized *A. muciniphila* when compared to that in ND-fed mice or in mice treated with Amuc_1100* (**Supplementary Fig. 4b**). *Naaa*, however, was not modified by any treatment in all intestinal segments (**Supplementary Fig. 4b–d**). Therefore, this set of data suggests that Amuc_1100* and pasteurized *A. muciniphila* exhibit distinct mechanisms of action on the endocannabinoid system.

Antimicrobial peptides are also contributing to the gut barrier function by shaping the gut microbiota[34]. We found that mice treated with pasteurized *A. muciniphila* had significantly higher *Lyz1* expression in both the jejunum and ileum when compared to ND-fed mice, while Amuc_1100* did not significantly affect this parameter (**Fig. 4d**,**e**). We observed a significantly lower *DefA* expression in the jejunum of mice treated with pasteurized *A. muciniphila* and Amuc_1100* as compared to ND-fed mice (**Fig. 4d**). In the ileum, mice treated with Amuc_1100* had significantly lower *DefA* expression than mice treated with either live or pasteurized *A. muciniphila* (**Fig. 4e**). This again suggests different mechanisms of action of Amuc_1100* and pasteurized *A. muciniphila*, in this case on antimicrobial peptides. However, treatment with *A. muciniphila* or Amuc_1100* did not change the HFD-mediated lower *Reg3g* and *Pla2g2* expression (**Fig. 4d**,**e** and **Supplementary Fig. 4e**). Altogether, these results suggest that Amuc_1100* and pasteurized *A. muciniphila* act on

Figure 3 *A. muciniphila* protein Amuc_1100* recapitulates the effects of the pasteurized bacterium on diet-induced obesity. (**a**–**d**) Stimulation of human HEK-Blue cells expressing (**a**) human TLR2, (**b**) TLR5, (**c**) TLR9 and (**d**) human NOD2 receptor. (**e**) Dynamic light scattering analysis of Amuc_1100* folding state according to the temperature. (**f**,**g**) Total body weight gain (**f**) and total fat mass gain (**g**) in grams after 5 weeks of treatment. (**h**) Daily food intake per mouse (g). (**i**) Plasma VLDL, LDL and HDL cholesterol (mg dl^{-1}). (**j**) Plasma triglycerides (mg dl^{-1}). (**k**) Plasma glucose (mg dl^{-1}) profile and (**l**) mean area under the curve (AUC) measured during an oral tolerance test (mg dl^{-1} min^{-1}). (**m**) Representative western blot of four total western blots for hepatic p-IRβ and β-actin with or without insulin stimulation. Ratio of the vehicle- and insulin-stimulated p-IRβ on the loading control measured by densitometry. (**n**) Representative western blot, of four total, for hepatic p-Akt^{thr308}, p-Akt^{ser473} and β-actin with or without insulin stimulation. Ratio of the vehicle- and insulin-stimulated p-Akt^{thr308} and p-Akt^{ser473} to the loading control measured by densitometry. Full-length blots are shown in **Supplementary Figures 6** and **7**. Data are presented as the mean ± s.e.m. Data in **a**,**c**,**d** represent three independent experiments, except for low concentrations of Amuc_1100* (0.05 and 0.5 μg/ml), where two independent experiments were performed. Data in **b** represent two independent experiments. Number of mice per group for **f**,**g**,**i**,**k**,**l**: ND: 9, HFD: 8, HFD live Akk synthetic: 8, HFD pasteurized Akk: 10, HFD Amuc_1100*: 10. For **h**, five measurements were obtained for each group. Number of mice per group for **j**: ND: 9, HFD: 8, HFD live Akk synthetic: 8, HFD pasteurized Akk: 10, HFD Amuc_1100*: 9. Number of mice per group for **m**,**n**: ND: 8, HFD: 9, HFD live Akk synthetic: 9, HFD pasteurized Akk: 9, HFD Amuc_1100*: 9. Data were analyzed using one-way ANOVA followed by Dunnett *post hoc* test versus DMEM condition for **a**,**c**,**d**, using Kruskal-Wallis followed by Dunn *post hoc* test versus DMEM condition for **b**, according to one-way ANOVA followed by Tukey *post hoc* test for **f**–**h**,**j**,**l**, and according to two-way ANOVA followed by Bonferroni *post hoc* test for **i**,**k**,**m**,**n**.*$P < 0.05$; **$P < 0.01$; ***$P < 0.001$.

different targets to reinforce the intestinal barrier in the jejunum and ileum; this could explain the correction of HFD-induced metabolic endotoxemia in treated mice.

Finally, we evaluated the safety and tolerability of *A. muciniphila* in individuals with excess body weight by treating them with different doses of live *A. muciniphila* (*Akk* synthetic, 10^{10} or 10^{9}) or pasteurized *A. muciniphila* (*Akk* pasteurized, 10^{10}) as part of an ongoing clinical study testing the efficacy of this bacterium on metabolic parameters associated with obesity and the metabolic syndrome. Subjects are currently being recruited and analyzed, and complete results will be reported once the study is complete (at the end of 2017). Anthropomorphic characteristics of the subjects at the beginning of treatment are reported in **Supplementary Table 1**. We analyzed several clinical parameters measured in probiotics safety assessments[35–37] before and after 2 weeks of treatment. No significant changes on markers related to inflammation and hematology, kidney, liver and muscle function were observed with any formulation of *A. muciniphila* (**Supplementary Fig. 5** and **Supplementary Table 2**). Moreover, the frequency of recorded adverse effects was similar in all groups (**Supplementary Table 3**). Borborygmi were reported by

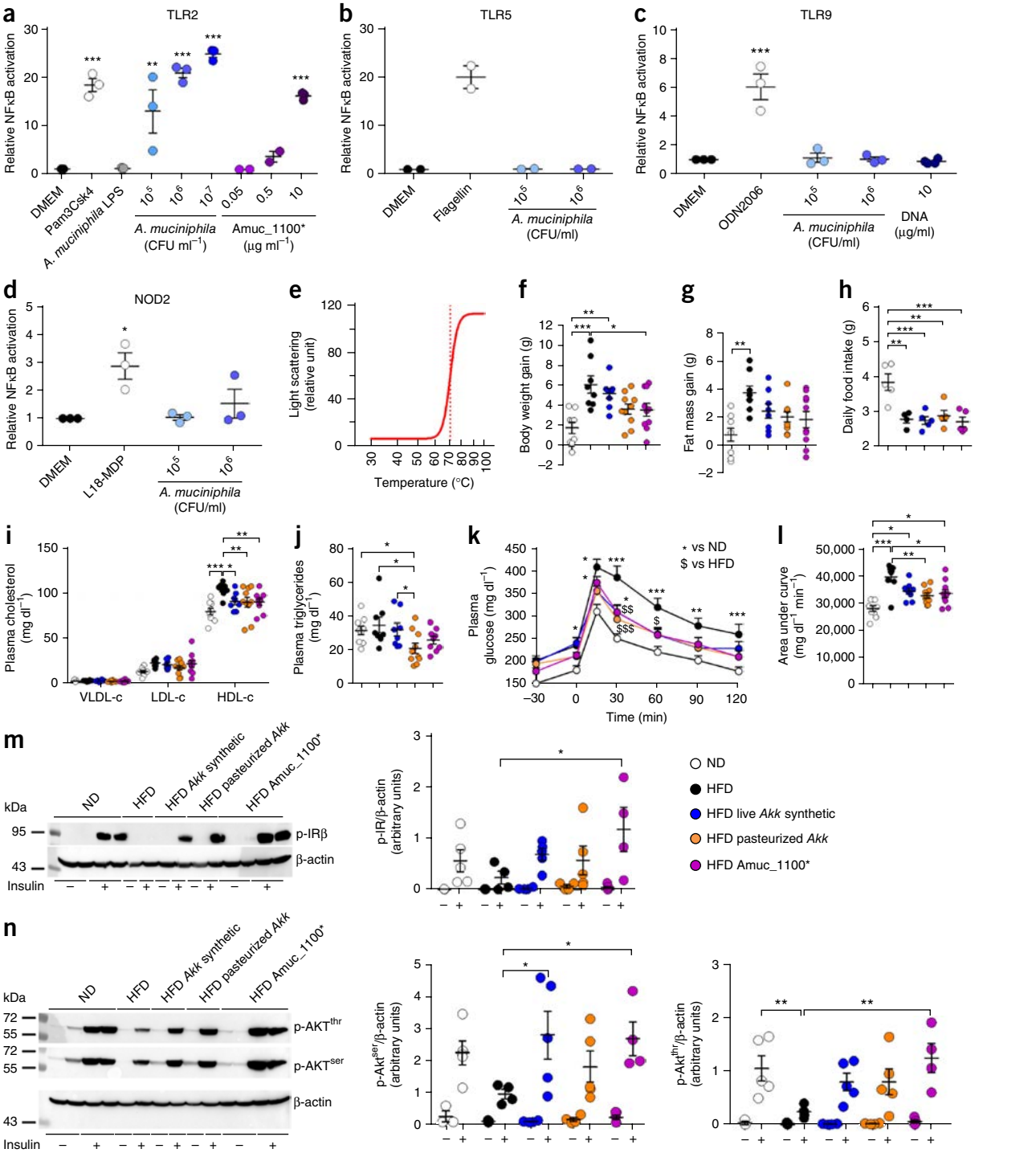

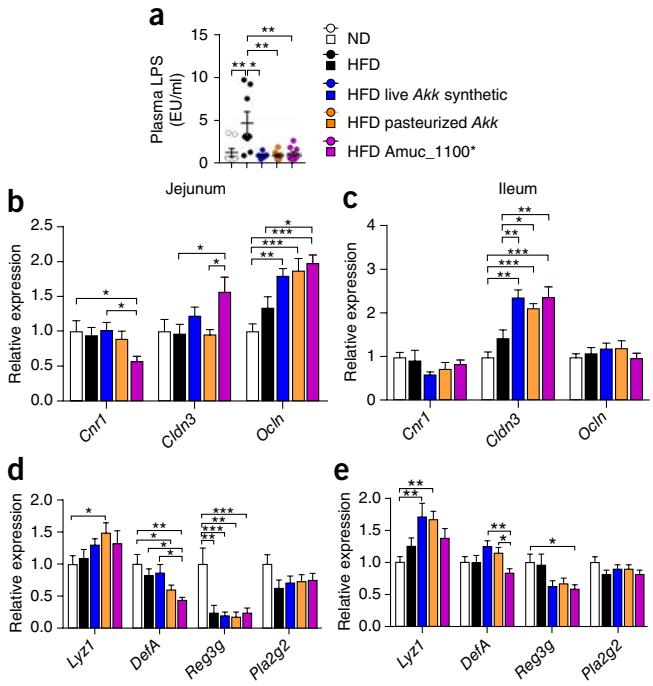

Figure 4 Effects of *A. muciniphila* or Amuc_1100* on the intestinal barrier function. (**a**) Portal plasma LPS (EU/ml). (**b**) Expression of *Cnr1*, *Cldn3* and *Ocln* in the jejunum. (**c**) Expression of *Cnr1*, *Cldn3* and *Ocln* in the ileum. (**d**) Expression of *Lyz1, DefA*, *Reg3g* and *Pla2g2* in the jejunum. (**e**) Expression of *Lyz1, DefA*, *Reg3g* and *Pla2g2* in the ileum. Data are presented as the mean ± s.e.m. Number of mice per group for **a**: ND: 8, HFD: 8, HFD live Akk synthetic: 5, HFD pasteurized Akk: 8, HFD Amuc_1100*: 9. Number of mice per group for **b** and **d**: ND: 8, HFD: 7, HFD live Akk synthetic: 8, HFD pasteurized Akk: 10, HFD Amuc_1100*: 9. Number of mice per group for **c** and **e**: ND: 9, HFD: 7, HFD live Akk synthetic: 8, HFD pasteurized Akk: 9, HFD Amuc_1100*: 9. Data were analyzed using one-way ANOVA followed by Tukey *post hoc* test. $^{*}P < 0.05$; $^{**}P < 0.01$; $^{***}P < 0.001$.

some subjects treated with live *A. muciniphila*, but the difference with other groups was not significant. While the number of subjects is limited, these first human data suggest that both live and pasteurized *A. muciniphila* are well tolerated in subjects with excess body weight and appear safe for oral administration in the context of obesity.

A. muciniphila is a promising target in the management of obesity and related disorders. Several studies have shown positive associations between *A. muciniphila* and the host metabolic health. Moreover, various dietary interventions targeting obesity and glucose intolerance increase *A. muciniphila* abundance[8,34,38], as does the glucose-lowering drug metformin[3,13]. To our knowledge, *A. muciniphila* is currently unique in the field of next-generation probiotic research as it resides in the mucus layer, a niche in close vicinity of host cells, and because it displays beneficial effects on several pathologies. Direct administration has proven protective not only against obesity but also against type 2 diabetes, gut barrier disturbances as well as atherosclerosis in various studies[8,13,14,22]. Moreover, metagenomics data suggest that *A. muciniphila* abundance could also be inversely associated with type 1 diabetes and inflammatory bowel disorders[39,40]. However, translational evaluation of *A. muciniphila* for human therapeutics is hampered by the requirement for animal-derived compounds in the growth medium of the bacterium. To circumvent this issue, we tested the effects of *A. muciniphila* grown on a synthetic medium compatible with human administration. We show in mice that effects on obesity and glucose metabolism are generally conserved when compared to the bacterium grown on a mucus-based medium.

Another hurdle to the use of live *A. muciniphila* in human subjects is its high sensitivity to oxygen. Here, we show that non-replicative, pasteurized *A. muciniphila* had stronger effects on body weight gain, fat mass gain and glucose intolerance in HFD-fed mice. These effects are associated with specific modulations of the host urinary metabolome, decreased intestinal energy absorption, normalization of plasma LPS concentration and decreased triglyceridemia. Moreover, we show that the outer membrane protein Amuc_1100* is involved in the *A.-muciniphila*-to-host interaction through TLR2 signaling, and that it partially recapitulates the effects of *A. muciniphila* against obesity, insulin resistance and gut barrier alteration. How pasteurization enhances the effects of *A. muciniphila* remains to be elucidated. The fact that Amuc_1100* is still stable at 70 °C suggests it could still be signaling in pasteurized cells and that pasteurization enhances the effects of *A. muciniphila* by increasing accessibility of this protein to the host. Whether this improvement of beneficial effects through pasteurization is specific to *A. muciniphila*, or could be extended to other bacteria, also needs to be tested. Regardless, pasteurization could represent an innovative way to use anaerobic strains as a therapeutic tool. Moreover, identification and isolation of specific bacterial products recapitulating all or part of the effects of the live organism could prove useful in the treatment of conditions such as inflammatory bowel diseases, where direct administration of live probiotics would be challenging.

Finally, preliminary human data suggest that treatment with either live or pasteurized *A. muciniphila* grown on the synthetic medium is safe in individuals with excess body weight, as no changes in relevant safety clinical parameters or reported adverse events were observed after two weeks of treatment. These results pave the way for future human studies investigating *A. muciniphila* as a therapeutic tool in the management of the metabolic syndrome.

METHODS

Methods, including statements of data availability and any associated accession codes and references, are available in the online version of the paper.

Note: Any Supplementary Information and Source Data files are available in the online version of the paper.

ACKNOWLEDGMENTS

We wish to thank A. Barrois, H. Danthinne, M. De Barsy, R.-M. Goebbels and T. Pringels for excellent technical assistance; S. Matamoros for helpful discussion and aid during tissue sampling; and the individuals who participated in this study. C. Druart's researcher position is supported by a FIRST Spin-Off grant from the Walloon Region (convention 1410053). Research in the Wageningen and Helsinki labs of W.M.d.V. was partially supported by ERC Advanced Grant 250172 (Microbes Inside), the SIAM Gravity Grant 024.002.002 and Spinoza Award of the Netherlands Organization for Scientific Research, and Grants 137389, 141140 and 1272870 of the Academy of Finland. P.D.C. is the recipient of grants from FNRS (convention J.0084.15, convention 3.4579.11), PDR (Projet de Recherche, convention: T.0138.14) and ARC (Action de Recherche Concertée–Communauté française de Belgique convention: 12/17-047). This work was supported by the FRFS-WELBIO under grant WELBIO-CR-2012S-02R. This work is supported in part by the Funds Baillet Latour (Grant for Medical Research 2015), a FIRST Spin-Off grant (FSO) from the Walloon Region, Belgium (convention 1410053) and FP7 METACARDIS (HEALTH-F4-2012-305312). P.D.C. is a recipient of POC ERC grant 2016 (European Research Council, Microbes4U_713547) and ERC Starting Grant 2013 (Starting grant 336452-ENIGMO).

AUTHOR CONTRIBUTIONS

P.D.C. and W.M.d.V. conceived the project. P.D.C. supervised the preclinical and clinical aspects, and W.M.d.V. the microbial culturing and expression. P.D.C. and

H.P. designed the mouse experiments, performed experiments and interpreted all the results, generated figures and tables and wrote the manuscript; A.E., C. Druart, M.V.H., L.G. and C. Depommier performed experiments. J.C., A.M. and M.-E.D. performed ^{1}H-NMR and UPLC-MS metabolomic analyses. N.M.D. provided reagents and analytic tools. T.D., L.L. and L.O.M. analyzed plasma lipoprotein profiles. C.B., K.C.H.v.d.A., H.P., C. Druart and S.A. performed the culturing and pasteurization of *A. muciniphila*. J.K. produced and purified Amuc_1100*, which was structurally analyzed by A.B. *In vitro* analysis of *A. muciniphila* and Amuc_1100* signaling was carried out by N.O. and C.B. J.-P.T., M.P.H., A.L., D.M., A.E., C. Druart, C. Depommier, W.M.d.V. and P.D.C. designed the clinical study. D.M., A.L., M.P.H. and J.-P.T., screened the subjects and contributed to follow-up. A.E., C. Druart, C. Depommier and P.D.C. followed subjects during the study. All authors discussed results and approved the manuscript.

COMPETING FINANCIAL INTERESTS

The authors declare competing financial interests: details are available in the online version of the paper.

1. Qin, J. *et al.* A metagenome-wide association study of gut microbiota in type 2 diabetes. *Nature* **490**, 55–60 (2012).
2. Le Chatelier, E. *et al.* Richness of human gut microbiome correlates with metabolic markers. *Nature* **500**, 541–546 (2013).
3. Forslund, K. *et al.* Disentangling type 2 diabetes and metformin treatment signatures in the human gut microbiota. *Nature* **528**, 262–266 (2015).
4. Ridaura, V.K. *et al.* Gut microbiota from twins discordant for obesity modulate metabolism in mice. *Science* **341**, 1241214 (2013).
5. Turnbaugh, P.J. *et al.* An obesity-associated gut microbiome with increased capacity for energy harvest. *Nature* **444**, 1027–1031 (2006).
6. Cani, P.D. *et al.* Metabolic endotoxemia initiates obesity and insulin resistance. *Diabetes* **56**, 1761–1772 (2007).
7. Everard, A. *et al.* Intestinal epithelial MyD88 is a sensor switching host metabolism towards obesity according to nutritional status. *Nat. Commun.* **5**, 5648 (2014).
8. Everard, A. *et al.* Cross-talk between *Akkermansia muciniphila* and intestinal epithelium controls diet-induced obesity. *Proc. Natl. Acad. Sci. USA* **110**, 9066–9071 (2013).
9. Derrien, M., Vaughan, E.E., Plugge, C.M. & de Vos, W.M. *Akkermansia muciniphila* gen. nov., sp. nov., a human intestinal mucin-degrading bacterium. *Int. J. Syst. Evol. Microbiol.* **54**, 1469–1476 (2004).
10. Collado, M.C., Derrien, M., Isolauri, E., de Vos, W.M. & Salminen, S. Intestinal integrity and *Akkermansia muciniphila*, a mucin-degrading member of the intestinal microbiota present in infants, adults, and the elderly. *Appl. Environ. Microbiol.* **73**, 7767–7770 (2007).
11. Derrien, M., Collado, M.C., Ben-Amor, K., Salminen, S. & de Vos, W.M. The mucin degrader *Akkermansia muciniphila* is an abundant resident of the human intestinal tract. *Appl. Environ. Microbiol.* **74**, 1646–1648 (2008).
12. Dao, M.C. *et al. Akkermansia muciniphila* and improved metabolic health during a dietary intervention in obesity: relationship with gut microbiome richness and ecology. *Gut* **65**, 426–436 (2016).
13. Shin, N.R. *et al.* An increase in the *Akkermansia* spp. population induced by metformin treatment improves glucose homeostasis in diet-induced obese mice. *Gut* **63**, 727–735 (2014).
14. Org, E. *et al.* Genetic and environmental control of host-gut microbiota interactions. *Genome Res.* **25**, 1558–1569 (2015).
15. Peng, G.C. & Hsu, C.H. The efficacy and safety of heat-killed *Lactobacillus paracasei* for treatment of perennial allergic rhinitis induced by house-dust mite. *Pediatr. Allergy Immunol.* **16**, 433–438 (2005).
16. Sakai, T. *et al. Lactobacillus plantarum* OLL2712 regulates glucose metabolism in C57BL/6 mice fed a high-fat diet. *J. Nutr. Sci. Vitaminol. (Tokyo)* **59**, 144–147 (2013).
17. Chevalier, C. *et al.* Gut microbiota orchestrates energy homeostasis during cold. *Cell* **163**, 1360–1374 (2015).
18. Dumas, M.E. *et al.* Metabolic profiling reveals a contribution of gut microbiota to fatty liver phenotype in insulin-resistant mice. *Proc. Natl. Acad. Sci. USA* **103**, 12511–12516 (2006).
19. Koeth, R.A. *et al.* Intestinal microbiota metabolism of L-carnitine, a nutrient in red meat, promotes atherosclerosis. *Nat. Med.* **19**, 576–585 (2013).
20. Bennett, B.J. *et al.* Trimethylamine-N-oxide, a metabolite associated with atherosclerosis, exhibits complex genetic and dietary regulation. *Cell Metab.* **17**, 49–60 (2013).
21. Miao, J. *et al.* Flavin-containing monooxygenase 3 as a potential player in diabetes-associated atherosclerosis. *Nat. Commun.* **6**, 6498 (2015).
22. Li, J., Lin, S., Vanhoutte, P.M., Woo, C.W. & Xu, A. *Akkermansia muciniphila* protects against atherosclerosis by preventing metabolic endotoxemia-induced inflammation in *Apoe*$^{-/-}$ mice. *Circulation* **133**, 2434–2446 (2016).
23. Shi, H. *et al.* TLR4 links innate immunity and fatty acid-induced insulin resistance. *J. Clin. Invest.* **116**, 3015–3025 (2006).
24. Abreu, M.T. Toll-like receptor signalling in the intestinal epithelium: how bacterial recognition shapes intestinal function. *Nat. Rev. Immunol.* **10**, 131–144 (2010).
25. Vijay-Kumar, M. *et al.* Metabolic syndrome and altered gut microbiota in mice lacking Toll-like receptor 5. *Science* **328**, 228–231 (2010).
26. Reunanen, J. *et al. Akkermansia muciniphila* adheres to enterocytes and strengthens the integrity of epithelial cell layer. *Appl. Environ. Microbiol.* **81**, 3655–3662 (2015).
27. Ottman, N. *et al.* Characterization of outer membrane proteome of *Akkermansia muciniphila* reveals sets of novel proteins exposed to the human intestine. *Front. Microbiol.* **7**, 1157 (2016).
28. Taniguchi, C.M., Emanuelli, B. & Kahn, C.R. Critical nodes in signalling pathways: insights into insulin action. *Nat. Rev. Mol. Cell Biol.* **7**, 85–96 (2006).
29. Liu, Z. *et al.* High-fat diet induces hepatic insulin resistance and impairment of synaptic plasticity. *PLoS One* **10**, e0128274 (2015).
30. Muccioli, G.G. *et al.* The endocannabinoid system links gut microbiota to adipogenesis. *Mol. Syst. Biol.* **6**, 392 (2010).
31. Cario, E., Gerken, G. & Podolsky, D.K. Toll-like receptor 2 controls mucosal inflammation by regulating epithelial barrier function. *Gastroenterology* **132**, 1359–1374 (2007).
32. Gu, M.J. *et al.* Barrier protection via Toll-like receptor 2 signaling in porcine intestinal epithelial cells damaged by deoxynivalnol. *Vet. Res.* **47**, 25 (2016).
33. Cani, P.D. *et al.* Endocannabinoids—at the crossroads between the gut microbiota and host metabolism. *Nat. Rev. Endocrinol.* **12**, 133–143 (2016).
34. Everard, A. *et al.* Microbiome of prebiotic-treated mice reveals novel targets involved in host response during obesity. *ISME J.* **8**, 2116–2130 (2014).
35. Jones, M.L., Martoni, C.J., Di Pietro, E., Simon, R.R. & Prakash, S. Evaluation of clinical safety and tolerance of a *Lactobacillus reuteri* NCIMB 30242 supplement capsule: a randomized control trial. *Requl Toxicol Pharmacol.* **63**, 313–320 (2012).
36. Burton, J.P. *et al.* Evaluation of safety and human tolerance of the oral probiotic *Streptococcus salivarius* K12: a randomized, placebo-controlled, double-blind study. *Food Chem. Toxicol.* **49**, 2356–2364 (2011).
37. Wind, R.D., Tolboom, H., Klare, I., Huys, G. & Knol, J. Tolerance and safety of the potentially probiotic strain *Lactobacillus rhamnosus* PRSF-L477: a randomised, double-blind placebo-controlled trial in healthy volunteers. *Br. J. Nutr.* **104**, 1806–1816 (2010).
38. Everard, A. *et al.* Responses of gut microbiota and glucose and lipid metabolism to prebiotics in genetic obese and diet-induced leptin-resistant mice. *Diabetes* **60**, 2775–2786 (2011).
39. Brown, C.T. *et al.* Gut microbiome metagenomics analysis suggests a functional model for the development of autoimmunity for type 1 diabetes. *PLoS One* **6**, e25792 (2011).
40. Png, C.W. *et al.* Mucolytic bacteria with increased prevalence in IBD mucosa augment in vitro utilization of mucin by other bacteria. *Am. J. Gastroenterol.* **105**, 2420–2428 (2010).

ONLINE METHODS

Culture and pasteurization of *Akkermansia muciniphila*. *A. muciniphila* MucT (ATTC BAA-835) was cultured anaerobically in a basal mucin-based medium as previously described[9], or in a synthetic medium where mucin was replaced by 16 g/l soy-peptone, 4 g/l threonine, and a mix of glucose and N-acetylglucosamine (25 mM each). Cultures were washed and concentrated in anaerobic PBS with 25% (vol/vol) glycerol under strict anaerobic conditions. Additionally, an identical quantity of *A. muciniphila* grown on the synthetic medium was inactivated by pasteurization for 30 min at 70 °C. Cultures were then immediately frozen and stored at −80 °C. A representative glycerol stock was thawed under anaerobic conditions to determine the CFU/ml by plate counting using mucin media containing 1% agarose (agar noble; Difco). Before administration by oral gavage, glycerol stocks were thawed under anaerobic conditions and diluted with anaerobic PBS to an end concentration of 2×10^8 CFU/150 µl and 2.5% glycerol.

Mice. Cohorts of 10- to 11-week-old male C57BL/6J mice (Charles River, L'Arbresle, France) were housed in a controlled environment (12 h daylight cycle, lights off at 6 p.m.) in groups of two mice per cage, with free access to food and water. Upon delivery, mice underwent an acclimation period of one week, during which they were fed a control diet (ND) (AIN93Mi, Research Diet, New Brunswick, NJ, USA). Mice were fed a normal chow diet (ND) (AIN93Mi, Research diet, New Brunswick, NJ, USA) or a high-fat diet (HFD) (60% fat and 20% carbohydrates (kcal/100g) D12492i, Research diet, New Brunswick, NJ, USA). Body weight, food and water intake were recorded once weekly. Body composition was assessed by using 7.5 MHz time domain-nuclear magnetic resonance (TD-NMR) (LF50 Minispec, Bruker, Rheinstetten, Germany). Mice experiments were not performed in a blinded manner.

For the first experiment, mice were treated daily with an oral administration of *A. muciniphila* grown on the mucus-based medium (HFD *Akk* M) or the synthetic medium (HFD *Akk* S). Additionally, one group of mice was treated daily with an oral administration of pasteurized *A. muciniphila* (HFD *Akk* P). Control groups (ND and HFD) were treated with an oral gavage of an equivalent volume of sterile PBS containing 2.5% glycerol. Treatment was continued for 4 weeks.

For the second experiment, mice were treated daily with an oral administration of either live or pasteurized *A. muciniphila* grown on the synthetic medium (HFD *Akk* S and HFD *Akk* P, respectively). Control groups (ND and HFD) were treated with an oral gavage of an equivalent volume of sterile PBS containing 2.5% glycerol. Treatment was continued for 5 weeks. Fresh urinary samples were collected during the final week of treatment and directly stored at −80 °C before analysis. Circulating leptin and resistin concentrations were determined using a multiplex immunoassay kit (Merck Millipore, Brussels, Belgium) and measured using Luminex technology (Bioplex, Bio-Rad, Belgium) following the manufacturer's instructions. Circulating adiponectin concentrations were determined using an ELISA kit (R&D Systems, Minneapolis, Minnesota, USA). Fecal energy content was measured on fecal samples harvested after a 24 h period during the final week of treatment by the use of a bomb calorimeter (Mouse Clinical Institute, Illkirch, France).

For the third experiment, mice were treated daily with an oral administration of either live or pasteurized *A. muciniphila* grown on the synthetic medium (HFD Akk S and HFD Akk P, respectively). Additionally, one group of mice was treated with a daily oral administration of 3 µg of the protein Amuc_1100* (see below) in an equivalent volume of sterile PBS containing 2.5% glycerol. This dose of Amuc_1100* was estimated to be equivalent to 1.5×10^8 CFU of *A. muciniphila* through the use of an in-house polyclonal antibody. Control groups (ND and HFD) were treated with an oral gavage of an equivalent volume of sterile PBS containing 2.5% glycerol. Treatment was continued for 5 weeks.

All mouse experiments were approved by and performed in accordance with the guidelines of the local ethics committee. Housing conditions were specified by the Belgian Law of May 29, 2013, regarding the protection of laboratory animals (agreement number LA1230314).

Exclusion criteria were predefined as follows: Mice displaying abnormal behavior when on a HFD (for example, increased aggressiveness leading to alteration of food intake and/or body weight loss) during the follow-up period were excluded from analyses. All tissues were carefully examined during necropsy and sampling. Any mouse displaying lesions (for example, granulous liver) was also excluded. Finally, for all analyses and for each group, any exclusion decision was supported by the use of the Grubbs test for outlier detection. Moreover, during the second experiment, two mice from the same cage in the group HFD *Akk* S were excluded from analysis of the OGTT and insulin data displayed in **Supplementary Figure 1d–g**, because of aggressiveness and fighting throughout the OGTT leading to abnormal blood glucose and insulin values.

Oral glucose tolerance test. 6-h-fasted mice were treated with an oral gavage glucose load (2 g glucose per kg body weight). Blood glucose was measured before oral glucose load and 15, 30, 60, 90 and 120 min after oral glucose load. Blood glucose was determined with a glucose meter (Accu Check, Roche, Switzerland) on blood samples collected from the tip of the tail vein.

Insulin resistance index. Plasma insulin concentration was determined on samples using an ELISA kit (Mercodia, Uppsala, Sweden) according to the manufacturer's instructions. Insulin resistance index was determined by multiplying the area under the curve of both blood glucose (−30 to 120 min) and plasma insulin (−30 and 15 min) obtained following the oral glucose tolerance test.

Tissue sampling. At the end of the treatment period, animals were anesthetized with isoflurane (Forene, Abbott, England) and blood was sampled from the portal and cava veins. After exsanguination, mice were killed by cervical dislocation. Subcutaneous adipose tissue depots, intestines and liver were precisely dissected, weighed and immediately immersed in liquid nitrogen and stored at −80 °C for further analysis.

Histological analyses. Subcutaneous adipose tissue (SAT) depots and ileal tissue were fixed in 4% paraformaldehyde for 24 h at room temperature. Samples were then immersed in ethanol 100% for 24 h before processing for paraffin embedding. For the determination of goblet cell density, ileal paraffin sections of 5 µm were stained with Periodic Acid Schiff (PAS) and counterstained with hematoxylin and eosin. Images were obtained using a SCN400 slide scanner and Digital Image Hub software (Leica Biosystems, Wetzlar, Germany). The number of goblet cells present on one villus was quantified and divided by the villus length. A minimum of 5 villi were analyzed per mouse in a blinded manner.

Urinary metabolomics analyses. Mouse urine samples were prepared and measured on a spectrometer (Bruker) operating at 600.22 MHz 1H frequency according to previously published protocol[41]; the 1H NMR spectra were then processed and analyzed as described previously[18].

UPLC-MS/MS determination of plasma TMA and TMAO concentrations. Ultra-Performance Liquid Chromatography-Tandem Mass Spectrometry (UPLC-MS/MS) was employed for the determination of plasma TMA and TMAO. Plasma samples (10 µL) were prepared as follows: I) samples were spiked with 10 µL Internal Standard (IS) solution ($^{13}C_3$/^{15}N-TMA, d_9-TMAO in water; 1 mg/l, Sigma-Aldrich). II) 45 µL of ethyl 2-bromoacetate solution (15g/l ethyl 2-bromoacetate, 1% NH4OH in acetonitrile) were added and derivatization of trimethylamines (TMA and $^{13}C_3$/^{15}N-TMA) to their ethoxy- analogs was completed after 30 min at room temperature. III) 935 µL of protein/lipid precipitation solution (94% acetonitrile/5% water/1% formic acid) was added; samples were centrifuged for 20 min (4 °C, 20,000g) and were transferred to UPLC-autosampler vials. Sample injections (5 µL loop) were performed to a Waters Acquity UPLC-Xevo TQ-S UPLC-MS/MS system equipped with an Acquity BEH HILIC (2.1 × 100 mm, 1.7 µm) chromatographic column. An isocratic elution was applied with 10 mM ammonium formate in 95:5 (v/v) acetronitrile:water for 7 min at 750 µl/min and 50 °C. Positive electrospray (ESI+) was used as ionization source and mass spectrometer parameters were set as follows: capillary, cone and sources voltages at −700, −18 and 50 V respectively, desolvation temperature at 600 °C, desolvation/cone/nebulizer gases were high purity nitrogen at 1000 l/hr, 150 l/hr and 7 bar respectively. Collision gas was high purity argon. Mass spectrometer was operated in multiple reactions monitoring (MRM) mode.

doi:10.1038/nm.4236

The monitored transitions were the following: for derivatized-TMA, +146 → +118/59 m/z (23/27 V); for derivatised-$^{13}C_3/^{15}N$-TMA, +150 → +63/122 m/z (27/22V); for TMAO, +76 → +59/58 m/z (12/13 V); for d_9-TMAO, +85 → +68/66 m/z (18/20 V). The system was controlled by the MassLynx software, also used for the data acquisition and analysis.

RNA preparation and real-time qPCR analysis. Total RNA was prepared from tissues using TriPure reagent (Roche). Quantification and integrity analysis of total RNA was performed by running 1 µl of each sample on an Agilent 2100 Bioanalyzer (Agilent RNA 6000 Nano Kit, Agilent). The cDNA was prepared by reverse transcription, and real-time qPCR was performed as previously described[8]. *RPL19* RNA was chosen as the housekeeping gene. Sequences of the primers used for real-time qPCR are available in **Supplementary Table 4**.

Production of Amuc_1100* protein. An expression plasmid for the production of His-tagged Amuc_1100, here termed Amuc_1100*, was constructed by amplification of its gene devoid of the coding sequence for its signal sequence and cloning of the resulting PCR product in pET-26b *E. coli* XL1Blue (Novagen, Merck Millipore, MA, USA). The following primer sequences were used for the construct: 5′-GGGTAC**CATATG**ATCGTCAATTCCAAACGC-3′ (Forward) and 5′-CCTTGG**CTCGAG**ATCTTCAGACGGTTCCTG-3′ (Reverse). Bolded sequences are restriction sites for NdeI and XhoI enzymes, respectively (Thermoscientific, MA, USA).

Conformation of the resulting plasmid pET-26b-1100 was verified by sequence analysis and transformed into *E. coli* BL21 (DE3). This strain was then grown in LB-broth containing kanamycin (50 µg/ml) with shaking at 220 rpm at 37 °C, followed by induction through the addition of 1 mM IPTG in the growth medium during mid-exponential phase. After three hours of induction, cells were pelleted by centrifuging 10 min at 5,000 g and cell pellets stored at −20 °C until lysis. Cell pellets were resuspended and lysed using lysozyme and sonification (Sonifier 450, Branson Ultrasonics Corporation, Danbury, CT, USA). Supernatant was collected after centrifugation and the Amuc_1100* protein purified by metal affinity purification under native conditions using Ni-16NTA His•Bind Resin (Novagen, Merck Millipore, MA, USA). After buffer exchange using a Zeba spin column, the protein content was determined (BCA assay; Pierce, Rockford, IL, USA) and the Amuc_1100* protein was stored at −20 °C.

Extraction of *A. muciniphila* LPS. *A. muciniphila* LPS was extracted using the hot phenol-water extraction method as described previously[42], with minor modifications. Briefly, bacterial cells from 5 ml overnight cultures were collected by centrifugation, washed once with water and resuspended into 500 µl of ultrapure water. The bacterial suspensions were warmed up at 65 °C and then mixed with an equal volume of water-saturated phenol preheated to 65 °C. The mixture was incubated at 65 °C for 10 min and then transferred to ice to cool down. After centrifugation at 4 °C for 5 min, the aqueous layer was carefully transferred to a new Eppendorf tube and the incubation with an equal volume of hot phenol was repeated twice. After this two volumes of acetone were added to the aqueous layer to precipitate LPS. The suspension was incubated at −20 °C for 2 h, after which it was centrifuged at 4 °C for 10 min and the pellet was dissolved in 50 µl of LPS-free water.

***In vitro* culture and stimulation of human HEK-Blue hTLR2/5/9/NOD2 cell lines.** For the immune receptor stimulation analysis HEK-Blue hTLR2, hTLR5, hTLR9 and hNOD2 cell lines (Invivogen, CA, USA) were used. Cells were authenticated by Invivogen. Presence of mycoplasma contamination was assessed regularly through a PCR-based method. Stimulation of the receptors with the corresponding ligands activates NF-κB and AP-1, which induces the production of secreted embryonic alkaline phosphatase (SEAP), the levels of which were measured by spectrophotometer (Spectramax, Molecular Devices, CA, USA). All cell lines were grown and subcultured up to 70–80% of confluency using as a maintenance medium Dulbecco's Modified Eagle Medium (DMEM) supplemented with 4.5 g/l D-glucose, 50 U/ml penicillin, 50 µg/ml streptomycin, 100 µg/ml Normocin, 2 mM L-glutamine and 10% (v/v) of heat-inactivated FBS. For each cell line, an immune response experiment was carried out by seeding HEK-blue cells in flat-bottom 96-well plates and stimulating them by addition of 20 µl bacterial suspensions. The 96-well plates were incubated for 20–24 h at 37 °C in a 5% CO_2 incubator. Receptor ligands Pam3CSK4 (10 ng/ml for hTLR2), RecFLA-ST (0.1 ng/ml for hTLR5), ODN 2006 (50 µM for hTLR9) and L18-MDP (0.1 ng/ml for hNOD2) were used as positive control whereas maintenance medium (DMEM) without any selective antibiotics was used as negative control. SEAP secretion was detected by measuring the OD600 at 1 h after addition of 180 µL of QUANTI-Blue (Invivogen) to 20 µL of induced HEK-Blue hTLR2/5/9/NOD2 supernatant.

Dynamic light scattering analysis. Heat induced aggregation of Amuc_1100* was measured by light scattering on a Carry Eclipse Fluorescence spectrophotometer (Agilent Biosciences, Santa Clara, CA, USA) equipped with Cary temperature controller and thermophobes. Amuc_1100* (at the concentration of 15 µM) was heated in presence of PBS (pH 7.4) at a constant rate of 1 °C/min from 30 °C to 100 °C. The light scattering at 350 nm was measured with excitation and emission slits at 2.5 nm.

Fast protein liquid chromatography. Plasma total cholesterol and triglycerides (TG) were measured with commercial kits (CHOD-PAP for cholesterol and GPO-PAP for TG; BIOLABO SA, Maizy, France). Separation of plasma lipoproteins was performed using fast protein liquid chromatography (FPLC, AKTA purifier 10, GE Healthcare, Chicago, IL, USA). 50 µl of individual plasma was injected and lipoproteins were separated on Superose 6 10/300GL column (GE Healthcare, Chicago, IL, USA) with NaCl 0.15 M at pH 7.4 as mobile phase at a 1 ml/min flow rate. The effluent was collected into fractions of 0.3 ml then cholesterol and TG content in each fraction were determined as described above. Quantification of cholesterol in lipoprotein classes (VLDL, LDL, and HDL) was performed by measuring the percentage peak area and by multiplying each percentage by the total amount of cholesterol.

Western blotting. To analyze the insulin signaling pathway in the third experiment, mice were allocated to either a saline-injected subgroup or an insulin-injected subgroup so that both subgroups were matched in terms of body weight and fat mass. They then received 1 mU insulin/g body weight (Actrapid; Novo Nordisk A/S, Denmark) under anesthesia with isoflurane (Forene, Abbott, England), or an equal volume of saline solution into the portal vein. Three minutes after injection, mice were killed and liver was harvested.

For detection of proteins of the insulin signaling pathway, tissues were homogenized in ERK buffer (Triton X-100 0.1%, HEPES 50 mM, NaCl 5 M, Glycerol 10%, $MgCl_2$ 1.5 mM and DTT 1 mM) supplemented with a cocktail of protease inhibitors and phosphatase inhibitors. Equal amounts of proteins were separated by SDS–PAGE and transferred to nitrocellulose membranes. Membranes were incubated overnight at 4 °C with antibodies diluted in Tris-buffered saline tween-20 containing 1% non-fat dry milk: p-IRβ (1:1,000; sc-25103, Santa Cruz, CA, USA), p-Akt^{Thr308} (1:1,000; #2965L, Cell Signaling, Danvers, MA, USA) and p-Akt^{Ser473} (1:1,000; #4060L, Cell Signaling). Quantification of phospho-proteins was performed on five animals with insulin injection and five animals with saline injection per group. The loading control was β-actin (1:10,000; ab6276).

Plasma LPS analysis. Portal vein plasma LPS concentration was measured using an Endosafe-Multi-Cartridge System (Charles River Laboratories, MA, USA), as previously described[8].

Safety assessment of live and pasteurized *A. muciniphila*. Results presented in this manuscript are *interim* safety reports from 20 subjects with excess body weight (Body mass index > 25 kg/m^2) presenting a metabolic syndrome following the NCEP ATP III definition (any three of the five following criteria: fasting glycaemia > 110 mg/dl, blood pressure ≥ 130/85 mmHg or antihypertensive treatment, fasting triglyceridemia ≥ 150 mg/dl, HDL cholesterol < 40 mg/dl for males, 50 mg/dl for females, and/or waist circumference > 102 cm for males, 88 cm for females). Subjects were voluntarily recruited from the Cliniques Universitaires Saint-Luc, Brussels, Belgium between December 2015 and May 2016. Subjects were assigned to any of the treatment arms following a randomized block design. The exclusion criteria were: presence of acute or

chronic progressive or chronic unstabilized diseases, alcohol consumption (> 2 glasses / day), previous bariatric surgery, any surgery in the 3 months before the study or planned in the next 6 months, pregnancy or pregnancy planned in the next 6 months, regular physical activity (> 30 min of sports 3 times a week), consumption of dietary supplements (omega-3 fatty acids, probiotics, prebiotics, plant stanols/sterols) in the month prior the study, inflammatory bowel disease or irritable bowel syndrome, diabetic gastrointestinal autonomic neuropathy (such as gastroparesis or reduced gastrointestinal motility), consumption of more than 30 g of dietary fibers per day, consumption of vegetarian or unusual diet, lactose intolerance or milk protein allergy, gluten intolerance, current treatment with medications influencing parameters of interest (glucose-lowering drugs such as metformin, DPP-4 inhibitors, GLP-1 receptor agonists, acarbose, sulfonylueras, glinides, thiazolidinediones, SGLT2 inhibitors, insulin, lactulose, consumption of antibiotics in the 2 months prior the study, glucocorticoids, immunosuppressive agents, statins, fibrates, orlistat, cholestyramine, or ezetimibe) and baseline glycated hemoglobin (HbA1c) > 7.5%. The Commission d'Ethique Biomédicale Hospitalo-facultaire from the Université catholique de Louvain (Brussels, Belgium) provided ethical approval for this study and written informed consent was obtained from each participant. The trial was registered at https://clinicaltrials.gov as NCT02637115.

Subjects were assigned to receive either a daily dose of placebo (an equivalent volume of sterile PBS containing glycerol), 10^{10} CFU live *A. muciniphila* (Akk S - 10^{10}), 10^{9} CFU live *A. muciniphila* (Akk S - 10^{9}), or 10^{10} CFU pasteurized *A. muciniphila* (Akk P - 10^{10}) for 3 months (placebo and bacteria were produced at a food-grade level according to the HACCP quality system). Blood samples were collected at the beginning of the treatment and a portion was directly sent to the hospital laboratory to measure relevant clinical parameters. Different tubes were used based on the clinical parameter: EDTA-coated tubes for white blood cell count, Sodium fluoride-coated tubes for fasting glycemia, citrate-coated tubes for clotting assays, and lithium-heparin-coated tubes for urea and enzymatic activities. After 2 weeks of treatment, subjects came back to the hospital for a safety visit, where blood samples were collected to allow comparison of clinical parameters to baseline values. Both the subjects and the physicians were blinded to the treatment.

Statistical analysis. Mouse data are expressed as the mean ± s.e.m. Number of mice allocated per group was based on previous experiments investigating the effects of *Akkermansia muciniphila* on diet-induced obesity[8]. At the beginning of each experiment, cages were randomly assigned to experimental groups to ensure that each group was matched in terms of body weight and fat mass. No blinding procedure was followed. Variance was compared using a Bartlett's test. If variances were significantly different between groups, values were normalized by Log-transformation before proceeding to the analysis. Differences between groups were assessed using one-way ANOVA, followed by the Tukey *post-hoc* test. In cases when variance differed significantly between groups even after normalization, a Kruskal-Wallis test was performed, followed by the Dunnett *post-hoc* test. A two-way ANOVA analysis with a Bonferonni *post-hoc* test was performed for the evolution of glycemia and insulinemia during the OGTT, for the repartition of cholesterol and triglycerides in specific lipoproteins and for Western-blot analyses.

In vitro data are expressed as the mean ± s.e.m. Variance was compared using a Bartlett's test. If variances were significantly different between groups, values were normalized by Log-transformation before proceeding to the analysis. Differences between groups were assessed using one-way ANOVA, followed by a Dunn *post-hoc* test comparing all conditions to DMEM. In cases when variance differed significantly between groups even after normalization, a Kruskal-Wallis test was performed. For the dynamic light scattering analysis of Amuc_1100*, a Boltzmann – Sigmoid curve was fitted to the data.

Human data are expressed as the mean ± s.d. Differences between groups were assessed using Kruskal-Wallis test. Differences between values observed at baseline and at the time of the safety visit were assessed using a Wilcoxon matched-pairs signed rank test. Data were analyzed using GraphPad Prism version 7.00 for Windows (GraphPad Software, San Diego, CA, USA).

Statistical comparisons were indicated with *, **, *** for $P < 0.05$, $P < 0.01$ and $P < 0.001$ respectively.

Data availability. The data that support the findings of this study are available from the corresponding author upon reasonable request.

41. Dona, A.C. *et al.* Precision high-throughput proton NMR spectroscopy of human urine, serum, and plasma for large-scale metabolic phenotyping. *Anal. Chem.* **86**, 9887–9894 (2014).
42. Zhang, L. & Skurnik, M. Isolation of an R^- M^+ mutant of *Yersinia enterocolitica* serotype O:8 and its application in construction of rough mutants utilizing mini-Tn5 derivatives and lipopolysaccharide-specific phage. *J. Bacteriol.* **176**, 1756–1760 (1994).

doi:10.1038/nm.4236